Li et al., http://dx.doi.org/10.1083/jcb.201602090

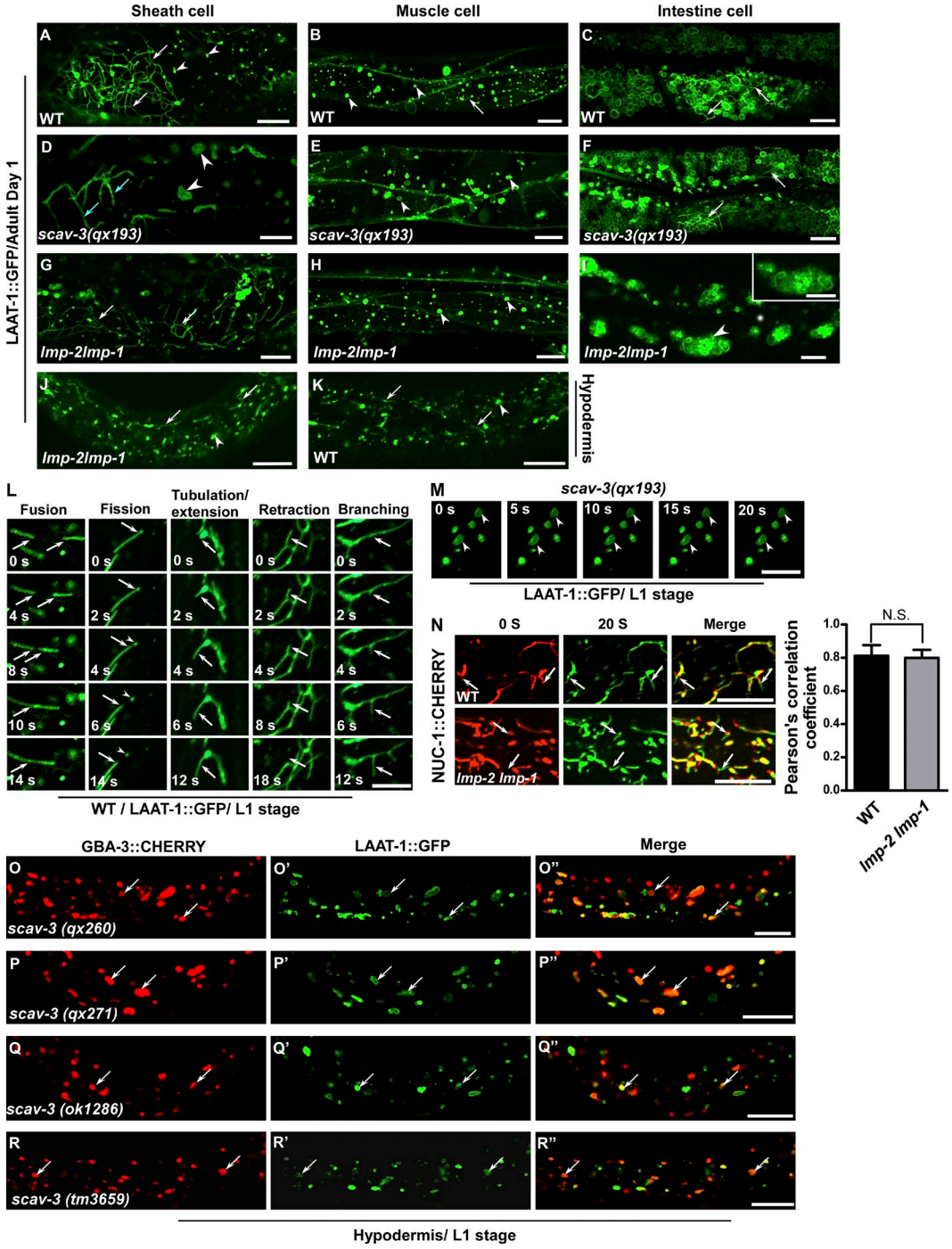

Figure S1. **Loss of *scav-3* affects lysosome morphology and dynamics.** (A–K) Confocal fluorescent images of wild-type (WT; A–C), *scav-3(qx193)* (D–F), and *lmp-2(tm6600) lmp-1(nr2045)* (G–I) adults or larvae (J and K) expressing LAAT-1::GFP in gonadal sheath cells, body wall muscles, intestine, and hypodermal cells. Arrowheads, globular lysosomes; arrows, tubular lysosomes; blue arrows, abnormally thick tubules in *scav-3(qx193)*. (L and M) Time-lapse images of lysosomes in the hypodermis of wild-type (L) and *scav-3(qx193)* (M) larvae expressing LAAT-1::GFP. Arrows indicate lysosomal changes that were followed and arrowheads designate static lysosomes in *scav-3(qx193)*. (N) Time-lapse images of lysosomes in the hypodermis of wild type and *lmp-2 lmp-1* expressing NUC-1::mCherry, with time point 0 s in red and 20 s in green. The overlay (merge) shows lysosome movement over time. Arrows indicate dynamic changes of lysosomes in wild type and *lmp-2 lmp-1*. Pearson's correlation coefficient was determined and is shown in the right panel. Data are shown as mean ± SD. At least 10 movies were analyzed in each strain. Data were compared with the unpaired *t* test. N.S., no significance. (O–R″) Confocal fluorescent images of the hypodermis in different *scav-3* mutant alleles expressing GBA-3::mCherry and LAAT-1::GFP. GBA-3::mCherry colocalizes with LAAT-1::GFP (arrows) in all *scav-3* mutant alleles. Bars, 10 µm.

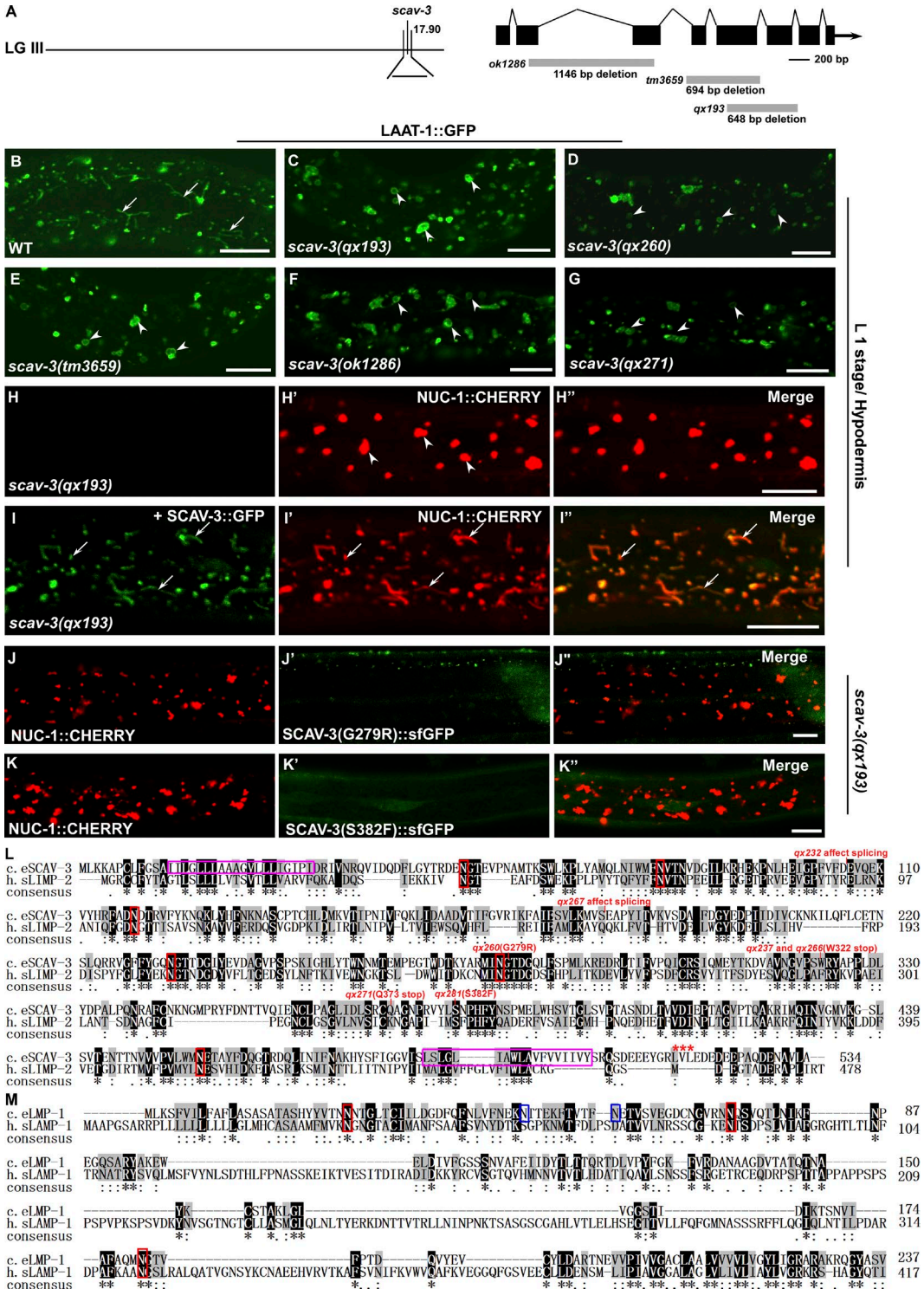

Figure S2. **Molecular cloning of *scav-3*.** (A) Cloning of *scav-3*. The left bar indicates the genetic position of *scav-3*. The *scav-3* gene structure is shown (right) with filled boxes representing exons and thin lines indicating introns. The arrow delineates the direction of transcription. The gray bars below the transcript show the size and position of the deleted regions in *ok1286*, *tm3659*, and *qx193*. (B–G) Confocal fluorescent images of the hypodermis in the indicated strains expressing LAAT-1::GFP. All *scav-3* alleles contained enlarged globular lysosomes (arrowheads) but lacked tubular structures (arrows). (H–I″) Confocal fluorescent images of the hypodermis in *scav-3(qx193)* carrying NUC-1::mCherry without (H–H″) or with (I–I″) expression of SCAV-3::GFP. Arrowheads and arrows indicate enlarged vesicular lysosomes and tubular structures, respectively. (J–K″) Confocal fluorescent images of the hypodermis in *scav-3(qx193)* expressing NUC-1::mCherry and SCAV-3(G279R)::sfGFP (J–J″) or SCAV-3(S382F)::sfGFP (K–K″). Both mutant SCAV-3 proteins fail to localize to lysosomes. (L) Sequence alignment of *C. elegans* (c.e) SCAV-3 and human (h.s) LIMP-2. Identical residues are shaded in black and similar ones in gray. Pink boxes indicate the two transmembrane domains. Mutations identified in different *scav-3* alleles are marked. The red asterisks delineate the amino acids important for the lysosomal targeting of SCAV-3, and the red boxes indicate putative glycosylation sites that are conserved in human LIMP-2. (M) Sequence alignment of *C. elegans* LMP-1 and human LAMP1. Identical residues are shaded in black and similar ones in gray. The red boxes indicate putative glycosylation sites that are conserved in human LAMP1, and the blue boxes designate sites that are not conserved. WT, wild type. Bars, 10 µm.

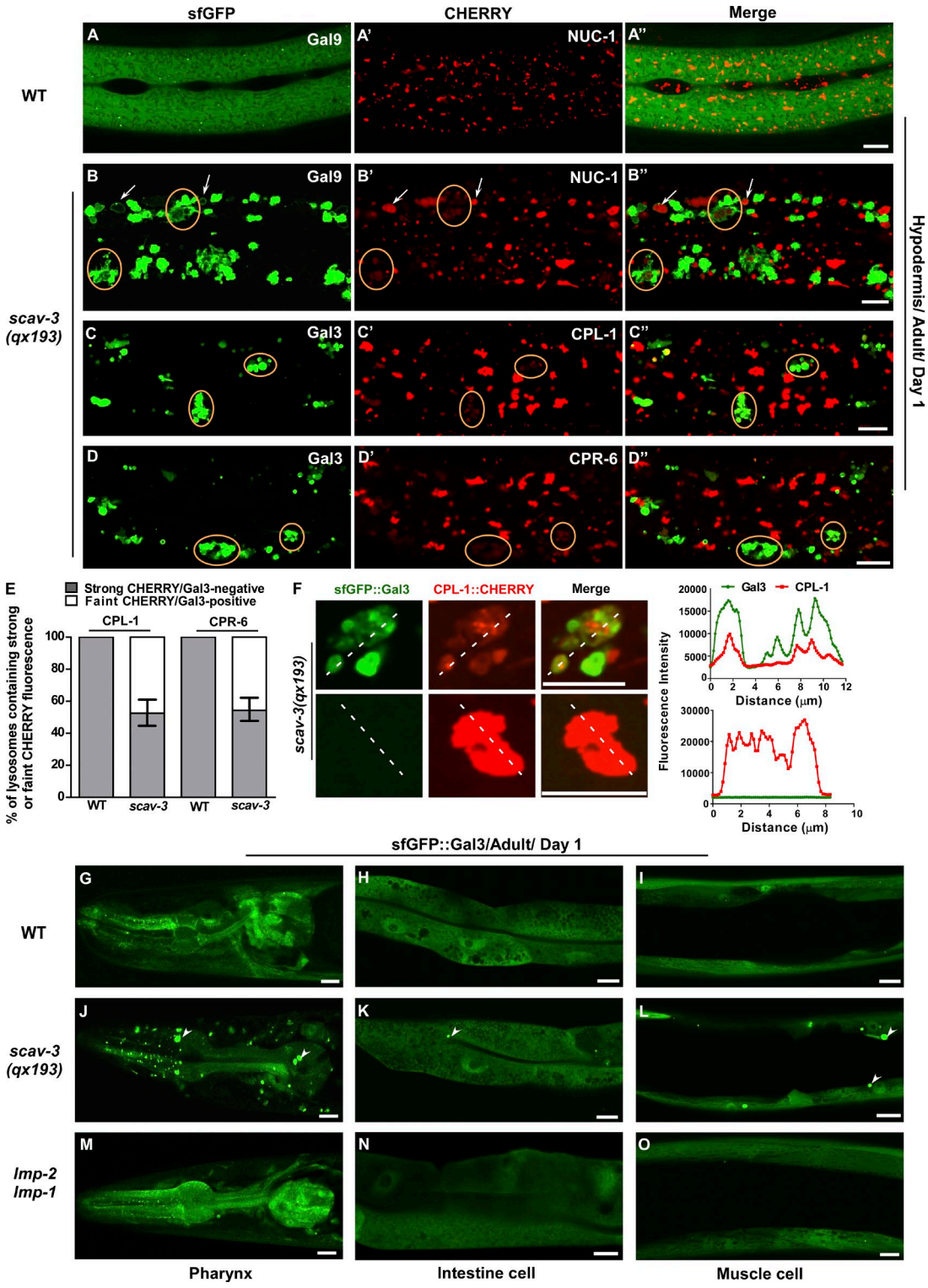

Figure S3. ***scav-3(qx193)* mutants accumulate damaged lysosomes.** (A–D″) Confocal fluorescent images of the hypodermis in wild-type (WT; A–A″) and *scav-3(qx193)* (B–D″) adults expressing NUC-1::mCherry and sfGFP::Galectin9 (Gal9; A–B″) or sfGFP::Gal3 and CPL-1::mCherry (C–C″) or CPR-6::mCherry (D–D″). sfGFP::Gal9- and sfGFP::Gal3-positive structures contain faint NUC-1::mCherry, CPL-1::mCherry, or CPR-6::mCherry fluorescence (circles), and sfGFP::Gal9 rings were seen around bright NUC-1::mCherry puncta (B–B″, arrows). (E) The percentage of lysosomes that contain strong mCherry fluorescence and are negative for GFP::Gal3 (intact) and those that contain faint mCherry fluorescence and are positive for GFP::Gal3 (damaged) was quantified in wild type and *scav-3(qx193)* expressing sfGFP::Gal3 and CPL-1::mCherry or CPR-6::mCherry. At least 15 animals were scored in each strain, and data are shown as mean ± SD. (F) Confocal fluorescent images and linescan analysis of lysosomes in *scav-3(qx193)* adults expressing sfGFP::Gal3 and CPL-1::mCherry. sfGFP::Gal3-positive structures contain faint CPL-1::mCherry fluorescence, whereas lysosomes with bright CPL-1::mCherry contained no sfGFP::Gal3 signal. At least 10 lysosomes were examined, and the representative result is shown. (G–O) Confocal fluorescent images of the pharynx (G, J, and M), intestine (H, K, and N), and body wall muscle (I, L, and O) in wild-type (G–I), *scav-3(qx193)* (J–L), and *lmp-2(tm6600) lmp-1(nr2045)* (M–O) adults expressing sfGFP::Gal3. Arrowheads indicate sfGFP::Gal3-positive structures. Bars, 10 μm.

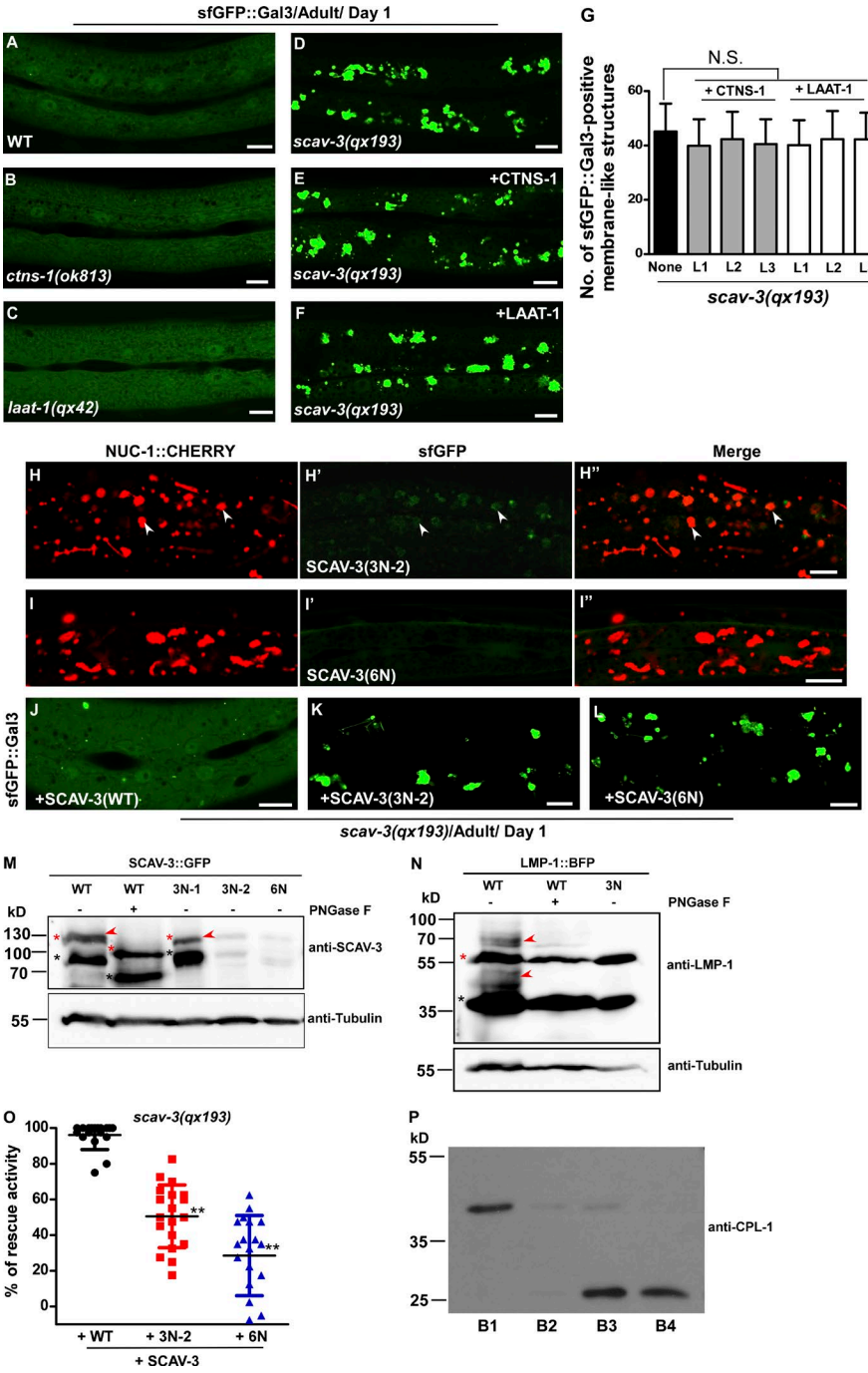

Figure S4. **Glycosylation is important for the stability and lysosomal targeting of SCAV-3.** (A–G) Confocal fluorescent images of the hypodermis in the indicated strains expressing sfGFP::Gal3 without (A–D) or with the expression of CTNS-1 (E) or LAAT-1 (F). Quantification is shown in G. Three independent transgenic lines of *scav-3(qx193)* expressing CTNS-1 or LAAT-1 (L1, L2, L3) were scored. (H–I″) Confocal fluorescent images of the hypodermis in *scav-3(qx193)* expressing NUC-1::mCherry and SCAV-3(3N-2)::sfGFP or SCAV-3(6N)::sfGFP, in which three and six glycosylation sites are mutated, respectively. Lysosomal localization is indicated by arrowheads. (J–L and O) Confocal fluorescent images of the hypodermis in *scav-3(qx193)* expressing sfGFP::Gal-3 and BFP fusion of SCAV-3 wild type (WT), SCAV-3(3N-2), or SCAV-3(6N). Expression of wild-type (WT) SCAV-3 but not SCAV-3(3N-2) or SCAV-3(6N) rescued the damaged lysosome phenotype in *scav-3(qx193)*. The percentage of rescue activity is quantified in O. At least 15 worms were scored in each strain. The distribution of the rescue activity is shown, and black lines represent the mean rescue activity (O). One-way ANOVA with Tukey's posttest was performed to compare all the other datasets with the wild-type SCAV-3. **, $P < 0.0001$. (M and N) Wild-type and mutant versions of SCAV-3 ::GFP (M) or LMP-1::BFP (N) that lack multiple glycosylation sites were expressed in *scav-3(qx193)*, then worm extracts were analyzed by Western blot using anti–SCAV-3 or anti–LMP-1 antibodies. PNGase F treatment was performed to remove the glycosylation of SCAV-3::GFP and LMP-1::BFP. The black and red asterisks indicate SCAV-3 or LMP-1 with or without the GFP or BFP fusion. The red arrowheads indicate the glycosylated proteins that are sensitive to PNGase treatment and may be affected in SCAV-3(3N-1) and LMP-1(3N). The protein levels of SCAV-3(3N-2)::GFP and SCAV-3(6N)::GFP were very low, likely because of the instability of the deglycosylated protein. The apparent molecular weight of LMP-1 (N, black asterisk) is bigger than its theoretical molecular weight and is not altered by PNGase treatment. (P) CPL-1 processing in lysosomes prepared from worms at day 1 of adulthood. The processing of CPL-1 is revealed by Western blot using anti–CPL-1 antibodies (full length, 38 kD; processed active form, 27 kD) and was used to determine the enrichment of lysosomes in different fractions (B1–4) separated by a density gradient as described in Materials and methods. Bars, 10 µm.

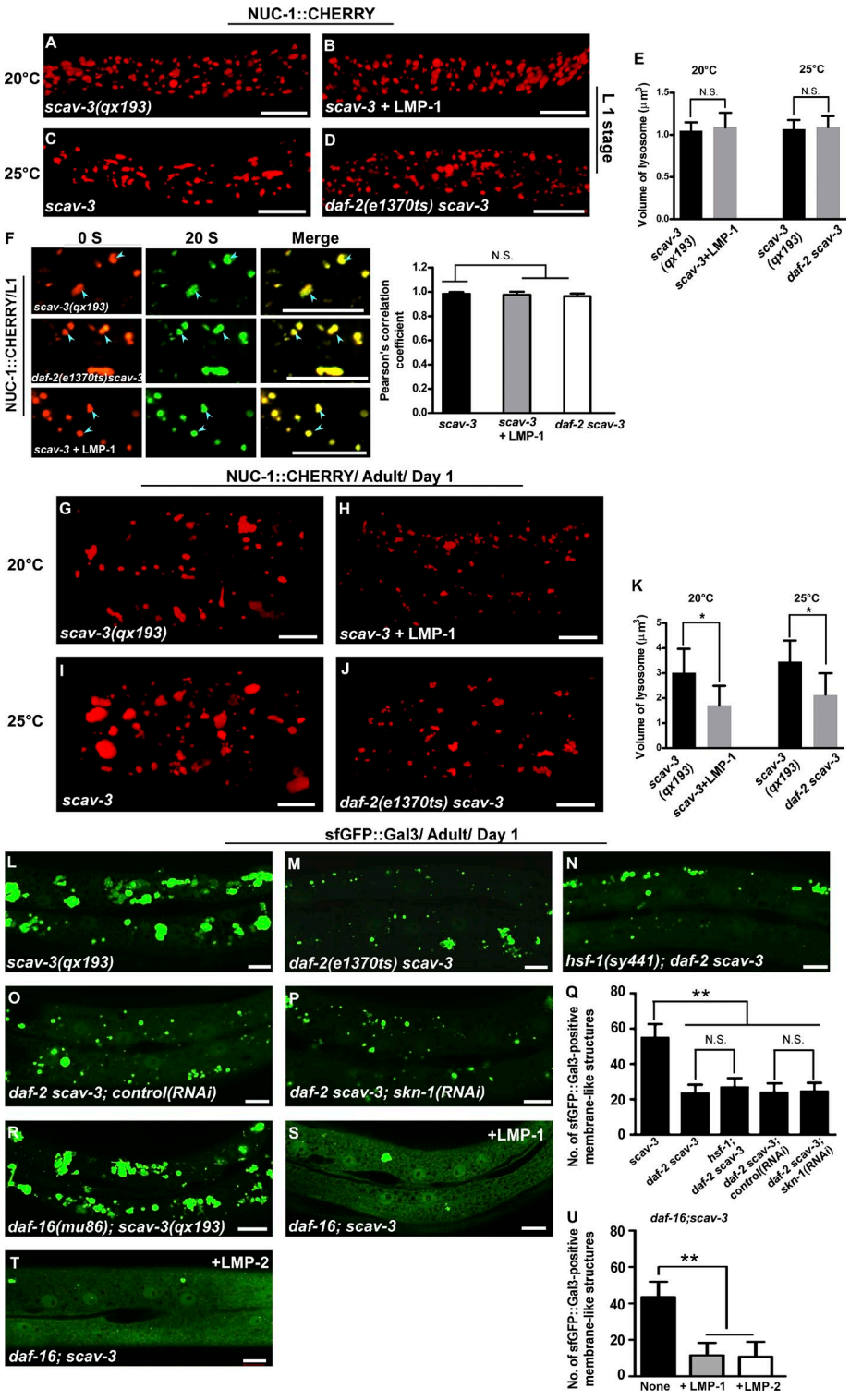

Figure S5. **The abnormal lysosome morphology and dynamics in *scav-3(qx193)* are not reversed by overexpression of LMP-1 or reduced activity of DAF-2.** (A–E and G–K) 3D reconstruction of lysosomes in the hypodermis of indicated strains expressing NUC-1::mCherry at L1 (A–D) and adult (G–J) stages. Lysosome volume is quantified in E and K. At least 10 worms were scored in each strain. Two-way ANOVA with the Bonferroni posttest was performed to compare datasets linked by lines. *, P < 0.05; N.S., no significance. (F) Time-lapse images of lysosomes in the hypodermis of L1 larvae expressing NUC-1::mCherry in *scav-3(qx193)*, *daf-2(e1370ts) scav-3*, or *scav-3* expressing LMP-1. Time point 0 s is in red and 20 s is in green. The overlay (merge) shows lysosome movement over time. Blue arrowheads indicate static vesicular lysosomes. Pearson's correlation coefficient was determined and is shown in the right panel. Data are shown as mean ± SD. At least 10 movies were analyzed in each strain. One-way ANOVA with Tukey's posttest was performed to compare datasets that are linked by lines. N.S., no significance. (L–U) Confocal fluorescent images of the hypodermis in the indicated strains expressing sfGFP::Gal3. In Q and U, the number of sfGFP::Gal3-positive membrane-like structures was quantified in hypodermal cell 7 (hyp7) of the indicated strains. At least 15 animals were scored in each strain, and data are shown as mean ± SD. One-way ANOVA with Tukey's posttest was performed to compare the datasets that are linked by lines. **, P < 0.0001; N.S., no significance. Bars, 10 μm.

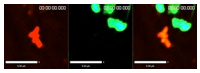

Video 1. **Appearance of damaged lysosomes in *scav-3* mutants expressing sfGFP::Gal3 and NUC-1::mCherry.** Lysosomes in the hypodermis of a *scav-3(qx193)* adult expressing NUC-1::mCherry and sfGFP::Gal3 are followed. sfGFP::Gal3 clusters around the NUC-1::mCherry vesicle, and its enrichment is accompanied by a gradual loss of mCherry fluorescence. Images were analyzed by time-lapse confocal microscopy using an inverted fluorescence microscope with an UltraView spinning-disc confocal scanner unit. The frames were taken every 1 min for 1–3 h, and selected frames are displayed every 1 s. Selected images are shown in Fig. 6 A.

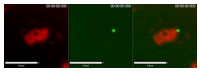

Video 2. **Appearance of damaged lysosomes in *scav-3* mutants expressing sfGFP::Gal3 and GBA-3::mCherry.** Lysosomes in the hypodermis of a *scav-3(qx193)* adult expressing GBA-3::mCherry and sfGFP::Gal3 are followed. sfGFP::Gal3 clusters around the GBA-3::mCherry vesicle, and its enrichment is accompanied by a gradual loss of mCherry fluorescence. Images were analyzed by time-lapse confocal microscopy using an inverted fluorescence microscope with an UltraView spinning-disc confocal scanner unit. The frames were taken every 1 min for 1–3 h, and selected frames are displayed every 1 s. Selected images are shown in Fig. 6 B.

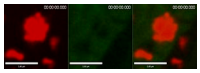

Video 3. **Appearance of damaged lysosomes in *scav-3* mutants expressing sfGFP::Gal3 and CPL-1::mCherry.** Lysosomes in the hypodermis of a *scav-3(qx193)* adult expressing CPL-1::mCherry and sfGFP::Gal3 are followed. sfGFP::Gal3 clusters around the CPL-1::mCherry vesicle, and its enrichment is accompanied by a gradual loss of mCherry fluorescence. Images were analyzed by time-lapse confocal microscopy using an inverted fluorescence microscope with an UltraView spinning-disc confocal scanner unit. The frames were taken every 1 min for 1–3 h, and selected frames are displayed every 1 s. Selected images are shown in Fig. 6 C.

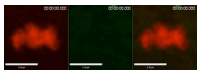

Video 4. **Appearance of damaged lysosomes in *scav-3* mutants expressing sfGFP::Gal3 and CPR-6::mCherry.** Lysosomes in the hypodermis of a *scav-3(qx193)* adult expressing CPR-6::mCherry and sfGFP::Gal3 are followed. sfGFP::Gal3 clusters around the CPR-6::mCherry vesicle, and its enrichment is accompanied by a gradual loss of mCherry fluorescence. Images were analyzed by time-lapse confocal microscopy using an inverted fluorescence microscope with an UltraView spinning-disc confocal scanner unit. The frames were taken every 1 min for 1–3 h, and selected frames are displayed every 1 s. Selected images are shown in Fig. 6 D.